Controlling the dimensionality in H bonded systems involving octahedral [Re6Qi8(CN)a6]4- and trans-[Re6Si8(CN)a4(H2O)a2]2- anions

A.Yu. Ledneva, N.G. Naumov, Nathalie Kyritsakas, S. Ferlay

Controlling the dimensionality in H bonded systems involving octahedral $[Re_6Q^i_8(CN)^a_6]^{4-}$ and *trans*-$[Re_6S^i_8(CN)^a_4(H_2O)^a_2]^{2-}$ anions

A.Yu. Ledneva[a], N.G. Naumov[a], N. Kyritsakas[b], S. Ferlay[b,*]

[a] Nicolaev Institute of Inorganic Chemistry SB RAS, 630090, 3 Acad. Lavrentiev Ave., Novosibirsk, Russia, e-mail ledneva@niic.nsc.ru
[b] Université de Strasbourg, CNRS, CMC UMR 7140, F-67000 Strasbourg, France, email: ferlay@unistra.fr

Abstract

The combination of cation of 1,4-diamidiniumbenzene hydrochloride ($H_2DAB{\cdot}Cl_2$) with $[Re_6Q_8(CN)_6]^{4-}$ (Q = S, Se) or $[Re_6S_8(CN)_4(OH)_2]^{4-}$ leads to solid-state compounds of formula $(H_2DAB)_2[Re_6Q_8(CN)_6]{\cdot}nH_2O$ (Q = S, n = 2.5 (**1**) or Q = Se, n = 2 (**2**)), and $(HDAB)_2[Re_6S_8(CN)_4(H_2O)_2]{\cdot}7H_2O$ **(3)**. Two isostructural compounds are formed through the monohapto recognition mode between H bond donors (H_2DAB^{2+}) and H bond acceptors (the –C≡N moieties of the cluster anions). A 2D system involving water molecules was formed, whereas with the disordered $[Re_6S_8(CN)_4(H_2O)_2]^{2-}$ anion, a deformed diamondoid porous compound was obtained. Moreover, amidinium cation becomes partially deprotonated ($HDAB^+$). These are rare examples of reliable charge assisted H bonded network involving Re cyanide clusters.

Keywords: rhenium cluster, cyanide, dications, H bonds, amidinium, Charge Assisted H-Bonding

1. Introduction

The obtaining of molecular materials with specific and targeted properties can be achieved using several approaches. The use of soft and reversible interactions enables a high modularity and processability and the formation of large crystals, useful for structure determination. This leads to compounds presenting optical, electric, magnetic, catalytic, zeolitic properties. In the field of weak and reversible bonds, the use of halogen bonds leads to molecular compounds presenting interesting mechanical properties, for example [1],[2]. For the formation of functional molecular compounds, the hydrogen bonds [3] have been extensively used, sometimes in combination with electrostatic interactions (Charge-Assisted Hydrogen Bonding, CAHB [4]), which allows the formation of robust molecular networks with reliable recognition patterns. The formation of H-bonded molecular networks has been well-documented during the last decades, with the formation of purely organic functional HOFs [5],[6]. In addition, the mastering of weak and reversible H bonds allows the formation of multicomponents "hybrid" hydrogen bonded networks (called sometimes "metallized HOFs") involving both inorganic (with reliable geometry, rigidity and introducing physical properties) and organic (presenting shape and structural versatility, flexibility) building blocks, leading to networks, displaying a wide range of properties [6]. While some examples are involving cationic metallic H bond donors [7], the formation of hydrogen bond-based hybrid (organic/inorganic) networks in the crystalline phase has been well illustrated, for example through the use of discrete mononuclear anionic cyanometallate [8],[9] or metal-oxalate derivatives [10],[11]. For mononuclear cyanometallate, the electron-donating potential of cyanometallate anions is not restricted to the formation of coordination bonds [12] and several material design strategies have been devoted on CAHB (Charged Assisted Hydrogen Bonding) involving cyanometallate based anions combined with organic hydrogen bond donors. Hexacyanoferrate(II) or Hexacyanoferrate(III), assembled with cationic N hydrogen bond donors bisamidinium derivatives leads to robust hydrogen bonded networks [13],[14],[15],[16]. Using $[M(CN)_2]^-$ (M=Ag or Au) anions, the reported compounds present luminescent properties [17],[18]. Multinuclear cyanometallate can also be used, and along this line, metallic clusters [19] appears to be candidates of choice due to their large size and rigid geometry. The multinuclear cyanometallate clusters $[Re_6Q_8(CN)_6]^{n-}$ (Q = S, Se, Te) have been used for the formation of coordination networks, "super Prussian blue" [20],[21],[22]. The $[Re_6Q_8(CN)_6]^{4-}$ (Q = S, Se or Te) [23],[24],[25],[26] and $[Re_6Q_8(CN)_4(OH)_2]^{4-}$ (Q = S, Se) [27],[28],[29] anions have been fully characterized from a structural point of view and

their electronic properties have been elucidated. They are also involved in H bonds: $(Ph_4P)_2(H)[Re_6Se_8(CN)_6]\cdot 8H_2O$ [30], $[(CH_3)C(NH_2)_2]_4[Re_6Se_8(CN)_6]$ [31], $[Zn(NH_3)_4]_2[Re_6Te_8(CN)_6]$ [32], $(EDT\text{-}TTF\text{-}CONH_2)_6[Re_6Se_8(CN)_6]$ [33],[34], $(Bu_4N)_2H[Re_6Te_8(CN)_6]\cdot 2H_2O$ or $H[cis\text{-}Fe(H_2O)_2][Re_6Se_8(CN)_6]\cdot 2H_2O$ [35], $[(H)\{Ln(H_2O)_4\}\{Re_6S_8(CN)_6\}]\cdot 2H_2O$ (Ln = Yb, Lu) [36] and metallomesogens based on Re_6 clusters [37].

In addition, in our group, we combined luminescent $[Re_6Q_8(CN)_6]^{4-}$ (Q = S or Se) with a non-emissive bisamidinium cation, providing a network in which the stabilization is mainly driven by H-bonds [38],[39]. Anions $[Re_6Q_8(CN)_4(OH)_2]^{4-}$ (Q = S, Se) also revealed to be embedded in strong H bonds networks [27],[40],[41].

Continuing our research of obtaining reliable and rationalizable hydrogen bonded networks, we intend to explore the formation of CAHB networks using a cationic rigid H bond donor species (cation of 1,4-diamidiniumbenzene), combined with rhenium cyano clusters $[Re_6Q_8(CN)_6]^{4-}$ (Q = S, Se) and also $[Re_6S_8(CN)_4(OH)_2]^{4-}$. Such cations are well known to form robust CAHB networks and have been encountered in many functional purely organic H bonded networks: porous networks [42],[43], compounds presenting proton conduction [44] or formation of radicals [45], and also involved in hybrid organic inorganic networks in metaloxallato [10],[11] and cyanocuprates [46].

Here below we will describe the 2D and 3D hybrid H-bonded networks that have been obtained using $[Re_6Q_8(CN)_6]^{4-}$ (Q = S, Se) or $[Re_6S_8(CN)_4(OH)_2]^{4-}$ combined with 1,4-diamidiniumbenzene. The formation of the observed structures could be rationalized.

1 Experimental Section

1.1 General Materials

$H_2DAB\cdot Cl_2$ (1,4-diamidiniumbenzene chloride) was obtained using the latest reported high yield synthesis [47]. $Cs_4[Re_6S_8(CN)_6]\cdot 3H_2O$ and $Cs_4[Re_6Se_8(CN)_6]\cdot 3H_2O$ were obtained by recrystallization from concentrated aqueous solution of $Cs_3K[Re_6S_8(CN)_6]\cdot 2H_2O$ [48] and $K_4[Re_6Se_8(CN)_6]\cdot 3.5H_2O$ [23] with twenty-fold excess of CsCl. $(Cs,K)_4[Re_6S_8(CN)_4(OH)_2]\cdot 2H_2O$ was synthesised as already reported [27].

1.2 Compounds synthesis

Compounds $(H_2DAB)_2[Re_6S_8(CN)_6]\cdot 2.5H_2O$ **(1),** $(H_2DAB)_2[Re_6Se_8(CN)_6]\cdot 2H_2O$ **(2)** and $(HDAB)_2[Re_6S_8(CN)_4(H_2O)_2]\cdot 7H_2O$ **(3)** were obtained using the same method: a 2 ml aqueous solution of organic $H_2DAB\cdot Cl_2$ (C = 7.5 mM) was layered in a thin tube on 3 ml of

aqueous solution of corresponding cluster (C = 0.5 mM) with addition of one drop of concentrated HCl. Yellow crystals suitable for X-ray diffraction were grew directly on the tube walls after few days. Yield 2–3 mg, ~ 40–50%.

(1) Anal. Calc for $C_{22}H_{33}N_{14}O_{2.5}Re_6S_8$ (air dried) : C, 13.85%; H, 1.74%; N, 10.28%; Found: C, 13.83%; H, 1.72%; N, 10.29%.

EDS: Re : S 6 : 7.9.

IR: υ(CN) 2117 cm^{-1}, also present all bands, corresponding to H_2DAB^{2+}.

(2) Anal. Calc for $C_{22}H_{32}N_{14}O_2Re_6Se_8$ (air dried): C, 11.62%; H, 1.42%; N, 8.62%; Found: C, 11.61%; H, 1.43%; N, 8.61%.

EDS: Re : Se 6 : 8.1.

IR: υ(CN) 2102 cm^{-1}, also present all bands, corresponding to H_2DAB^{2+}.

(3) Anal. Calc for $C_{20}H_{42}N_{12}O_9Re_6S_8$ (air dried): C, 12.20%; H, 2.15%; N, 8.54%; Found: C, 12.20%; H, 2.22%; N, 8.54%.

EDS: Re : S 6 : 7.8.

IR: υ(CN) 2106 cm^{-1}, also present all bands, corresponding to $HDAB^{+}$.

1.3 Characterization of the compounds

The characterizations have been performed on polycrystalline samples.

FT-IR spectra were recorded on a Perkin Elmer ATR spectrometer.

Elemental analyses were performed by the Service de Micro-analyses de la Federation de Recherche Chimie of the University de Strasbourg.

The EDS analysis was performed with a high-resolution JEOL JSM 6700F scanning electron microscope with an energy-dispersive analyser of the chemical composition.

Thermogravimetric analysis (TGA) was carried out with NETZSCH TG 209 F1 Iris Thermo Microbalance Instrument, (He flow 30 ml/min in an Al_2O_3 crucible, heating rate 10 °C/min in the temperature range 30 – 600 °C).

Optimization of the geometric parameters of organic fragment H_2DAB^{2+} ($C_8H_{14}N_4$), $HDAB^{+}$ ($C_8H_{13}N_4$) and neutral DAB ($C_8H_{12}N_4$) were performed using the density functional theory in the software package AMS2022 [49]. The calculations of IR spectra were carried out in the TZP all-electronic basis [50] using the GGA BP86 functional [51]. The zero-order regular approximation (ZORA) was used in all calculations in this work to take into account the scalar relativistic effects [52].

Crystallography

For all the compounds, the data were collected at 173(2) K on a Bruker APEX8 CCD diffractometer equipped with an Oxford Cryosystem liquid N_2 device, using graphite-monochromated MoKα (λ= 0.71073 Å) radiation. The refinement and all further calculations were carried out using SHELXL-2014 [53] (for **2**) and SHELXL-2017 (for **1** and **3**) [54]. The H-atoms were included in calculated positions and treated as riding atoms using SHELXL default parameters. For **1** and **2** the O1 atom of the water molecule, corresponding to an electron density of ~8 (1) or 8.7 (**2**) e/A^3, is located in a void with no acceptor. The closest O1-Q contact is 3.5 (Q = S, **1**) or 3.6 (Q = Se, **2**) Å. In addition, O1 also acts an acceptor for the NH bond of the cation (N4 atom).

For **3**, N4 atom belongs to disordered CN group with s.o.f equal to 0.5. The hydrogen atoms of the solvate water molecules in **3** have not been included in the structure refinement due to the strong disorder of the water molecules in the voids of the structure. The structure refinement bias (WGHT) can be improved by removing solvent water molecules (SQUEEZE). The non-H atoms were refined anisotropically, using weighted full-matrix least-squares on F^2. A semi-empirical absorption correction was applied using SADABS in APEX2 [55]. Pore volume was calculated using the PLATON program [56].

CCDC Numbers for $(H_2DAB)_2[Re_6S_8(CN)_6]\cdot 2.5H_2O$: 2326357, $(H_2DAB)_2[Re_6Se_8(CN)_6]\cdot 2H_2O$: 2326356 and $(HDAB)_2[Re_6S_8(CN)_4(H_2O)_2]\cdot 7H_2O$: 2326355. Crystal data and structure refinement parameters are listed in Table 1.

Powder diffraction studies (XRPD)

Diagrams were collected on polycrystalline samples, on a Bruker D8 diffractometer using monochromatic Cu-Kα radiation with a scanning range between 4 and 40° using a scan step size of 8° mn^{-1}. The calculated XRPD diagrams were obtained using PCW software [57] on cif file of **1**.

2 Results and discussion

$[Re_6Q_8(CN)_6]^{4-}$ (Q = S or Se) anions present six pendant terminal –C≡N groups, orthogonally disposed at the vertices of the octahedral Re_6 cluster [58], whereas $[Re_6S_8(CN)_4(OH_2)_2]^{2-}$ [27] presents two neutral OH_2 terminal groups located in *trans* position and the four –C≡N ligands are located in the basal plane (Figure 1a). The average distances between the nitrogen atoms of –C≡N groups within cluster are around 7 Å for –C≡N groups in *cis* position and 10 Å for the groups in *trans* position for $[Re_6Q_8(CN)_6]^{4-}$ (Q = S, Se) and $[Re_6S_8(CN)_4(OH_2)_2]^{2-}$.

DAB derivatives are rigid spacer between the protonated amidine moieties, and the average distances between the N atoms of linked amidinium moieties are 7 Å in the flat model (Figure 1b) [44]. This feature appears unfavourable for the regular dihapto recognition mode through H bond between the donors and acceptors, that is frequently encountered in discrete mononuclear anionic cyanometallate combined with amidinium moieties [8].

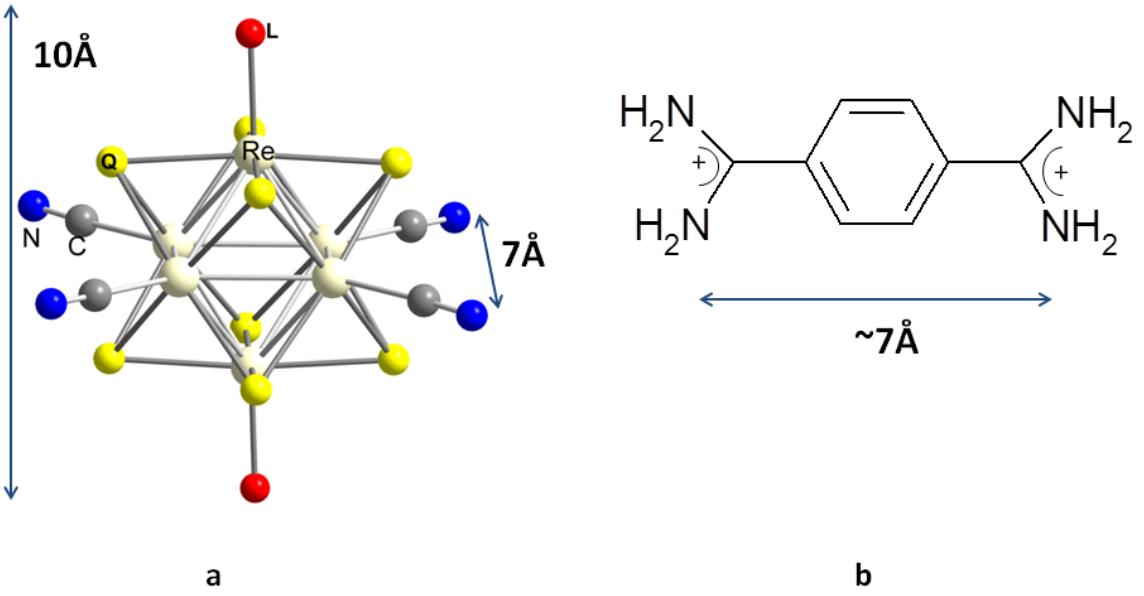

Figure 1. Structures and their metrics of a) Cluster anions $[Re_6Q_8(CN)_4L_2]^{4-}$ (Q = S, Se; L = CN or OH) and b) the organic cation H_2DAB^{2+}.

Using usual techniques for forming suitable single crystals for XRD (slow diffusion), three single crystalline compounds were obtained (see experimental part). A series of two isostructural 2D H bonded compounds was obtained with $[Re_6Q_8(CN)_6]^{4-}$, presenting the formula $(H_2DAB)_2[Re_6Q_8(CN)_6]\cdot nH_2O$ (Q = S or Se) and a 3D H bonded compound was obtained when combining $H_2DAB\cdot Cl_2$ with $[Re_6S_8(CN)_4(OH)_2]^{4-}$ in acidic media presenting the formula $(HDAB)_2[Re_6S_8(CN)_4(H_2O)_2]\ ]\cdot 7H_2O$.

Both structures are described here below. In all cases, the anion/cation stoichiometry is 1/2. The geometry of the $[Re_6Q_8(CN)_6]^{4-}$ (Q = S or Se) and $[Re_6S_8(CN)_4(H_2O)_2]^{2-}$ anions and also within H_2DAB^{2+} are not discussed: the observed distances and angles are corresponding to what is usually observed in such species (see distances in the Table 2).

2.1 Structure of $(H_2DAB)_2[Re_6Q_8(CN)_6]\cdot nH_2O$ (Q = S (1) or Se (2))

The combination of $H_2DAB\cdot Cl_2$ with $[Re_6Q_8(CN)_6]^{4-}$ (Q = S or Se), leads to the formation of two isomorphous and isometric compounds (see crystallographic Table, Table 1)

of formula $(H_2DAB)_2[Re_6Q_8(CN)_6]\cdot nH_2O$ (Q = S, n = 2.5 (**1**) or Q = Se, n = 2 (**2**)). The H bonded compounds can be described as a 2D H-bonded system, where a plane is presented in figures 2a and 2b.

The structure of compound (**2**) will be described here below, since the distances for (**1**) can be found in Table 2. In the unit cell, one can find two protonated cations H_2DAB^{2+}, one $Re_6Se_8(CN)_6]^{4-}$ anion and two water molecules. In the cation, the C–N in H_2DAB^{2+} are in the 1.29-1.33Å range (see Table 2), which corresponds well to the distances in the fully protonated dication $H_2DAB\cdot Cl_2$ (1.305(3)-1.317(4)Å) [59]. Each $[Re_6Se_8(CN)_6]^{4-}$ anionic cluster is surrounded by eight cations oriented as shown in figure 2d: as already mentioned, the recognition mode between cations (amidinium moieties) and anions is in monohapto mode. It means that each of the 6 pendant C ≡N moieties of $[Re_6Se_8(CN)_6]^{4-}$ are interacting at least with one dication, and for two of them with two cationic moieties, with N···N distances in the 2.944(8)-3.071(8) Å range, as shown in Table 2. On the other side, each dication is surrounded by 4 anions as shown in figure 2c. It is interesting to note, that from one side of each cation, the NH_2^+ moieties are interacting with two anions, in bifurcated H bonds, and on the other side, one of the N atoms is not involved in H bonds, and the other is involved in a H bond with a water molecule with a $N\cdots O_W$ distance of 2.895(8) Å. As a consequence, a 2D compound is formed, the layer is located the *x*O*y* plane, and the anions being surrounded on each side, along the *a* axis, with parallelly organised cations. In the interlayer space, one can find water molecules, but the water molecules are pointing at the surface of the formed planes, and are not gluing the planes together, parallel stacked along the *c* axis. The replacement of Se atoms by S (or comparing structure of **2** and structure of **1**) leads to small increase of the free space between the cluster anions, and thus 0.5 water molecule (per unit cell) can be additionally introduced (as seen form the general formula). The $O_{1w}\cdots N$ distance for oxygen atom with fully occupancy is 2.914(6) Å while $O_{2w}\cdots N$ (0.5 occupancy) is 3.033(5) Å. The shortest contacts $O_{1w}\cdots Q$ is 3.82 Å (Q = S, **1**) against 3.71 Å (Q = Se, **2**) and $O_{1w}\cdots N{\equiv}C$ is 3.315 Å, $O_{2w}\cdots N{\equiv}C$ 3.73 Å for compound **1** against $O_w\cdots N{\equiv}C$ 3.51 Å for **2**.

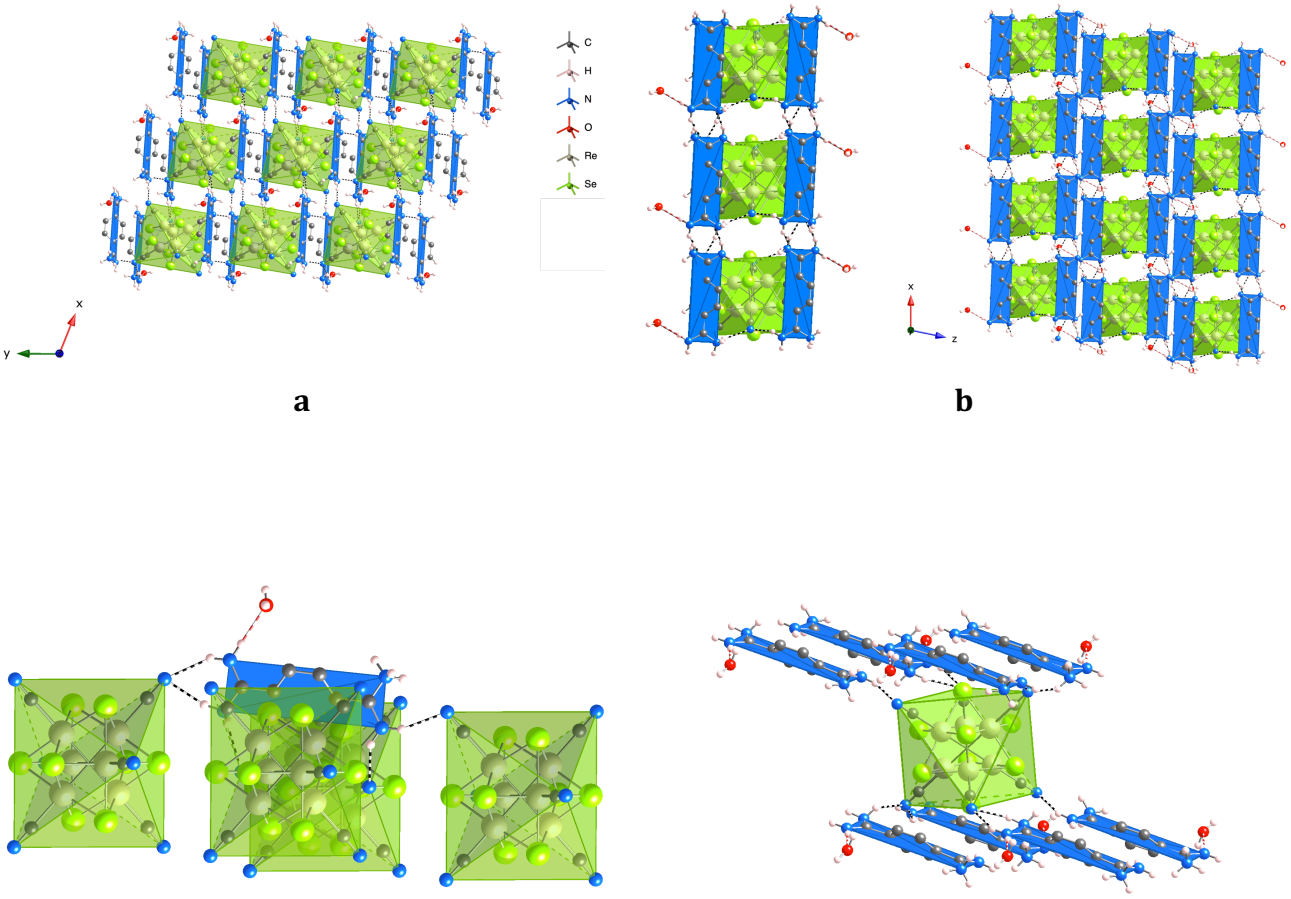

Figure 2. Structure of (**2**), (a) The layered structure in the *x*O*y* plane; (b) a plan viewed along the *a* axis, and the stacking of the planes in the *x*O*z* plane, along the *c* axis.(c) the surrounding around H_2DAB^{2+} dication (d) the surrounding around the $[Re_6Se_8(CN)_6]^{4-}$ anions; (Black dashed lines are representing hydrogen N···N bonds between cluster and cations and red dashed lines are representing hydrogen N···O bonds between cations and water molecules). The $[Re_6Se_8(CN)_6]^{4-}$ clusters is depicted as green octahedra, the H_2DAB^{2+} – blue plane.

2.2 Structure of $(HDAB)_2[Re_6S_8(CN)_4(H_2O)_2]\cdot 7H_2O$ (3)

The combination of $H_2DAB\cdot Cl_2$ with $[Re_6S_8(CN)_4(OH)_2]^{4-}$ should lead to the formation of a compound with formal formula "$(H_2DAB)_2[Re_6S_8(CN)_4(OH)_2]$". It is well-known that in acidic solution (for the synthesis, pH is about 1), the cluster anion $[Re_6S_8(CN)_4(OH)_2]^{4-}$ is protonated and turns into $[Re_6S_8(CN)_4(H_2O)]^{2-}$ form [29]. The $[Re_6S_8(CN)_4(H_2O)_2]^{2-}$ anion in **(3)** presents two H_2O terminal groups located in *trans*

position, and disordered on 4 positions of the basal plane of the octahedron; thus only two pendant terminal –C≡N moieties are located without ambiguity on the cluster in apical positions. In the unit cell, one can find two organic amidinium moeties per one cluster anion. In the cation, the C–N distances are equal to 1.252(11)Å and 1.350(11)Å, which is very close to the distances in the neutral fragment Benzdiamidine (deprotonated DAB) (1.283(3)Å and 1.349(4)Å) [60], we can then assume that the cation is partially deprotonated with a +1 formal charge, $HDAB^{+}$. Thus, the final formula of compound (**3**) is $(HDAB)_2[Re_6S_8(CN)_4(H_2O)_2]\cdot 7H_2O$. Also 7 water molecules have been refined into the porous structure, without strong interaction with the H bonded network (figure 4 b).

Each $[Re_6S_8(CN)_4(H_2O)_2]^{2-}$ anionic cluster is surrounded by eight cations, and this presents the same coordination pattern as in the case of 1 and **2**, with different orientations of the dications around the metallic anions (figure 3).

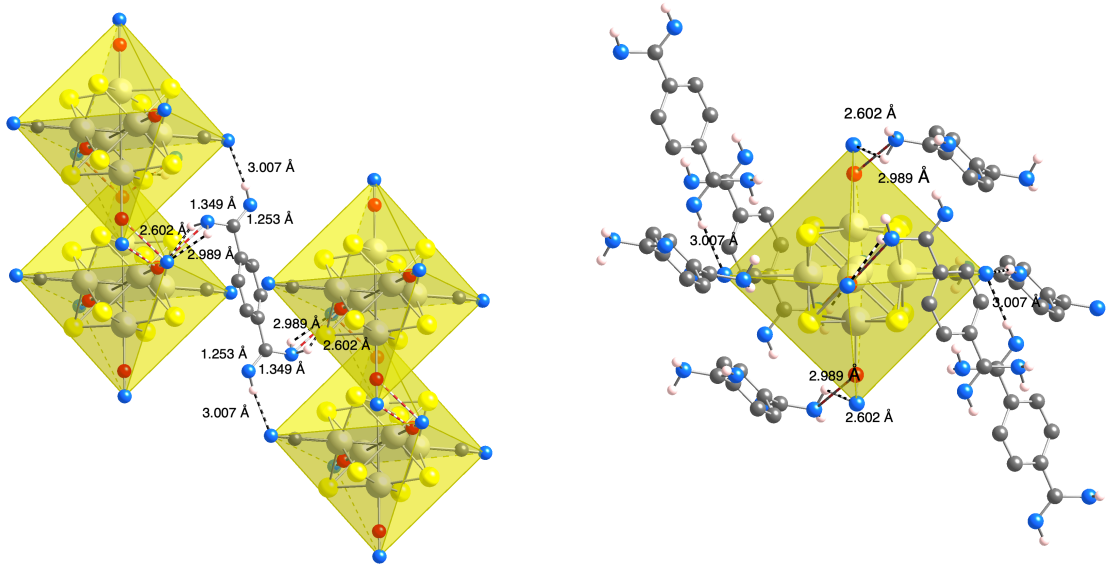

a **b**

Figure 3. For (**3**), (a) the surrounding around $HDAB^{+}$; (b) the surrounding around the $[Re_6S_8(CN)_4(H_2O)_2]^{2-}$ anions. (Black dashed lines are representing hydrogen N···N bonds between clusters and cations and red dashed lines are representing hydrogen N···O bonds between pendant C ≡N and aqua)

On the other side, each cation is surrounded by 4 anions as shown in figure 3a, and the four N donating atoms are involved in N···N (2.602(17) and 3.007(9) Å). There are also $HN\cdots OH_2$ (2.989(12) Å) H-bonds in the structure of **(3)** (see distances in Table 2). The H bonded compound can be described as a 3D H-bonded system (figure 4 a). An additional interesting point is that there are interactions between the clusters through C ≡N···HOH

(2.947(12) Å) between aqua and pendant C ≡N moieties and also through O···O (3.374(8) Å) H-bonds (H_2O···HOH bonds). The 3D deformed diamondoid porous system is formed with short contacts between the clusters in along the *b* direction, and as a consequence the formed channel pores are relatively large, with a diameter of *ca* 14 Å (see blue spheres in figure 4a). The channel walls are formed by N4 of the disordered cyano group (and its oxygen), N3 of another cyano group, N1 of the cation and S3 of the anion. Total potential solvent area volume per unit cell is 2278.4 $Å^3$, it is about 25.2% of all volume. These pores are filled with disordered water molecules, forming thus an extended hydrogen bonds as shown in figure 4 b.

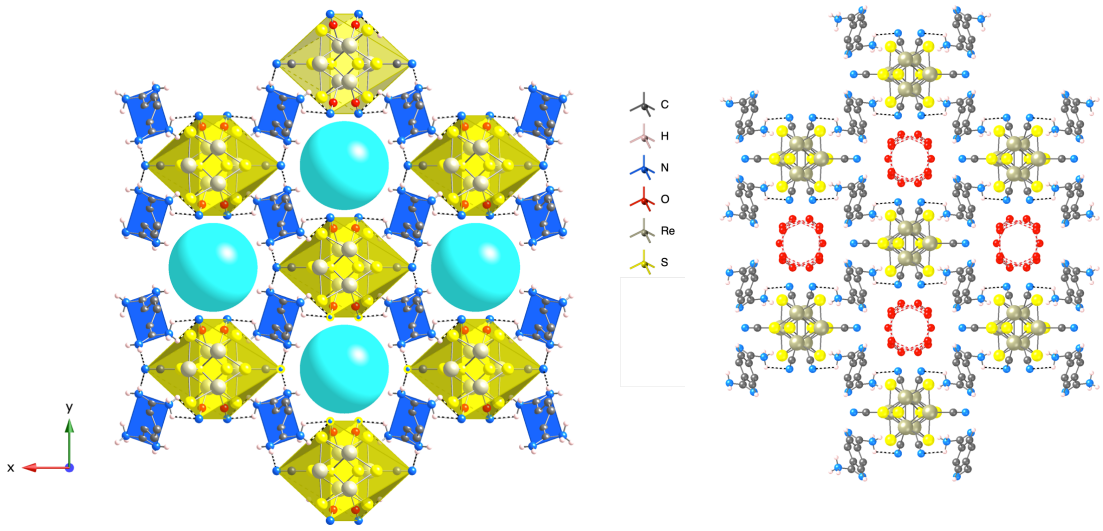

a **b**

Figure 4 a and b. For (**3**), the porous 3D structure (light blue spheres represent the pores); (Black dashed lines are representing hydrogen N···N bonds between clusters and cations and red dashed lines are representing hydrogen N···O bonds between pendant C ≡N and aqua, blue spheres are representing the pores).

Table 2. Crystallographic table for (**1**)-(**3**) recorded at 100K

	(**1**)	(**2**)	(**3**)
Chemical formula	$C_{22}H_{33}N_{14}O_{2.5}Re_6S_8$ '$C_6N_6Re_6S_8$, 2($C_8H_{14}N_4$), 2.5(H_2O)'	$C_{22}H_{32}N_{14}O_2Re_6Se_8$ '$C_6N_6Re_6Se_8$, 2($C_8H_{14}N_4$), 2(H_2O)'	$C_{20}H_{42}N_{12}O_9Re_6S_8$ '$C_4N_4Re_6S_8O_2H_4$, 2($C_8H_{13}N_4$) 7(H_2O)'
Formula weight, g/mol	1907.30	2273.49	1842.22
Crystal size, mm	0.040 x 0.040 x 0.050	0.030 x 0.030 x 0.040	0.050 x 0.060 x 0.060
Crystal system	triclinic	triclinic	monoclinic
Space group	*P* -1	*P* -1	*C* 2/m
Unit cell dimensions, Å	*a* = 9.9424(2) *b* = 10.4860(2) α = 102.4740(10)° β = 96.9380(10)° γ = 110.5610(10)°	*a* = 9.7896(5) *b* = 10.6636(4) α = 104.8140(10)° β = 95.8230(10)° γ = 108.6870(10)°	*a* = 19.5782(13) *b* = 14.6650(9) *c* = 8.2219(6) β = 105.170(3)°
Volume, $Å^3$	989.59(3)	1028.42(8)	2278.4(3)
Z	1	1	2
Density (calculated), g/cm^3	3.185	3.671	2.849
Absorption coefficient, mm^{-1}	18.742	24.707	16.295
F(000)	861	1000	1764
Theta range for data collection	2.01 to 30.00°	1.96 to 28.71°	1.76 to 28.84°
Index ranges	–14<=*h*<=13, –11<=*k*<=14, –14<=*l*<=14	–13<=*h*<=12, –10<=*k*<=14, –14<=*l*<=14	–26<=*h*<=17, –16<=*k*<=19, –11<=*l*<=11
Reflections collected	22569	10164	3068
Independent reflections	5672 [*R*(int) = 0.0333]	4871 [*R*(int) = 0.0228]	3068 [*R*(int) = 0.0232]
Max. And min. Transmission	0.5220 and 0.4470	0.5210 and 0.4370	501.0000 and 0.4350
Data / restraints / parameters	5672 / 3 / 243	4871 / 4 / 243	3065 / 0 / 117
GOOF on F^2	1.049	1.011	1.050
Δ/σ_{max}	0.001	0.015	0.001
Final R indices	4650 data; I>2σ(I) R_1 = 0.0202, wR_2 = 0.0413 all data R_1 = 0.0254, wR_2 = 0.0432	4012 data; I>2σ(I) R_1 = 0.0274, wR_2 = 0.0628 all data R_1 = 0.0360, wR_2 = 0.0668	2618 data; I>2σ(I) R_1 = 0.0274, wR_2 = 0.0673 all data R_1 = 0.0355, wR_2 = 0.0717
Weighting scheme	w=1/[$\sigma^2(F_o^2)$+(0.0228P)^2+1.4613P] where P=(F_o^2+2F_c^2)/3	w=1/[$\sigma^2(F_o^2)$+(0.0322P)^2+0.2564P] where P=(F_o^2+2F_c^2)/3	w=1/[$\sigma^2(F_o^2)$+(0.0345P)^2+2.1950P] where P=(F_o^2+2F_c^2)/3
Largest diff. Peak and hole, $eÅ^{-3}$	0.718 and –0.868	2.252 and –2.139	2.249 and –1.025
R.M.S. deviation from mean, $eÅ^{-3}$	0.199	0.280	0.209

Table 2. Selected bond length for **1-3**, min–max, average, Å

	(**1**) $(H_2DAB)_2[Re_6S_8(CN)_6]\cdot 2.5H_2O$	(**2**) $(H_2DAB)_2[Re_6Se_8(CN)_6]\cdot 2H_2O$	(**3**) $(HDAB)_2[Re_6S_8(CN)_4(H_2O)_2]\cdot 7H_2O$
Re–Re	2.5962(2)–2.6034(2), 2.5998(2)	2.6272(3)–2.6364(3), 2.6337(3)	2.5922(3)–2.5987(4) 2.5950(4)
Re–Q (Q = S or Se)	2.4006(11)–2.4138(12) 2.4074(11)	2.5151(6)–2.5331(7), 2.5234(6)	2.4092(13)–2.4203(12), 2.4146(13)
Re–C	2.108(5) –2.115(4), 2.112(5)	2.103(6)–2.113(6), 2.109(6)	2.113(8)
Re-O	–	–	2.092(4)
C–N (in H_2DAB^{2+} or $HDAB^{+}$)	1.292(6)–1.318(6), 1.308(6)	1.289(8)– 1.328(7) 1.307(8)	1.252(11) 1.350(11)
C ≡N···H-N	2.926(6)–3.092(6), 2.996(7)	2.944(8)– 3.071(8), 2.982(8)	2.602(17) 3.007(9)
N···Ow	2.914(6) 3.033(5)	2.895(8)	-

2.3 XRPD data

The XRPD data of $(H_2DAB)_2[Re_6Q_8(CN)_6]\cdot nH_2O$ (Q = S, n = 2,5 (**1**) or Q = Se, n = 2 (**2**)) microcrystalline compounds have been recorded. They are presented in figures 5, and compared to the calculated diagram for **1**. They are showing that the powdered samples are polycrystalline.

The diagram of $(HDAB)_2[Re_6S_8(CN)_4(H_2O)_2]\cdot 7H_2O$ **(3)** is not presented, there are not a good matching between the experimental and canculated diagrams. We assume that the compound partially loses water molecules when exposed to the air, which is confirmed by TGA analysis data, according to which only about 3 solvent water are removed.

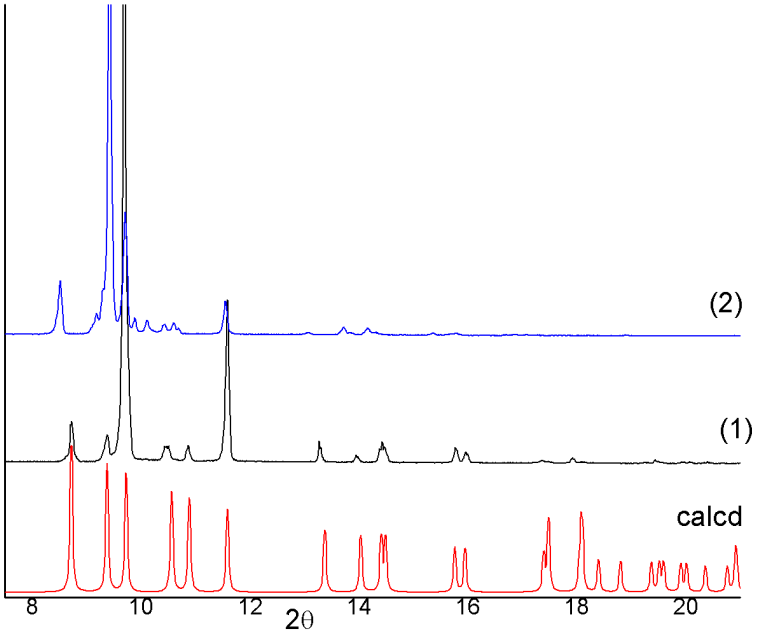

Figure 5. Comparison of the simulated (calcd, bottom line, for compound **1**) and experimental powder X-Ray diffraction studies (XRPD) diagrams for isostructural (**1**) and (**2**) (Q = S and Se).

2.4 IR Spectra

The experimental IR spectra of (**1**) and (**3**) are presented, compared to the calculated ones of H_2DAB^{2+}, $HDAB^{+}$ and DAB (figure 6) (see details for calculations in the experimental section), in order to determinate the protonation state of the cation. For (**1**) and (**3**) vibrations of υ(C ≡N), organic fragment and water molecules, involved in H bonding appear in the same region. However, it is worth noting that the spectrum of compound **3** in the region of 3600–3000 cm^{-1} looks more complicated. The valence vibration υ(N-H) in **(3)** (3628 cm^{-1}) is shifted to a higher frequency region compared to the ones observed for (**1**) (3600cm^{-1}) and is closer to the one observed for the monoprotonated form of the cation (3597 cm^{-1}) than the one observed for the dication (3542 cm^{-1}). The total amount of bands of symmetric and asymmetric υ(N-H) in this region also increased for (**3**), it is linked to the non-equivalence of (NH_2) and (NH) groups in the organic fragment. The stretching vibrations υ(OH) of water molecules (solvated and coordinated) are also located in this region. For example, bands around 3300 cm^{-1} can be assigned to υ_a(N-H) for H-N=C group of monocation and to the υ(OH_2) vibrations. The bending vibrations of water δ(HOH) are located near 1600-1630 cm^{-1} almost the same as δ(HNH) in cations (1660-1600 cm^{-1}). Thus, it is difficult to determine exactly how these bands are influenced by the hydrogen bonding in compounds (**1**)–(**3**) because of their strong overlap with the bands corresponding to the organic cations.

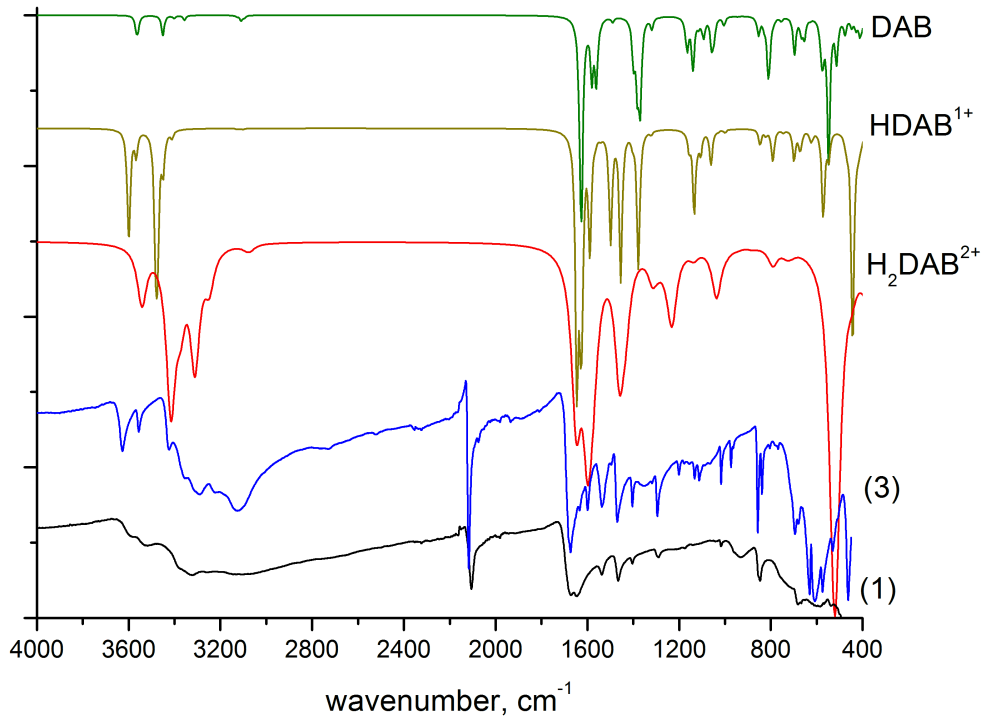

Figure 6. calculated IR spectra of H_2DAB^{2+}, $HDAB^{+}$ and DAB (three upper lines) and experimental IR spectra of compound (**3**) (blue line) and compound (**1**) (bottom black line).

2.5 TGA characterization

The thermal decomposition of compounds (**1**)–(**3**) was studied by the TG method (see TG curves on Figure 7). The total mass loss occurs in two steps for compounds (**1**) and (**2**), corresponded to the removal of water molecules about 100–180°C, ~2% (**1,** calcd 1.90%) and 1.5% (**2,** calcd 1.58%)) and organic cation (in a range 300–400°C, ~17,5% (**1,** calcd 17.51%) and 14.5% (**2,** calcd 14.62%)).

The decomposition of **3** occurs in a more complex way. The process of removing solvate water molecules smoothly turns into the removal of cations and coordinated water molecules and further cluster decomposition. The TGA diagrams show a clear difference between **1, 2** and **3**, the broader plateau of **1, 2** (160–280°C) compared with **3** indicating a higher thermal stability for the 2D networks. At the first stage about ~2 % of mass loss occurs, that can correspond to 3 water molecules instead of 7. Presumably, **3** quickly loses some of solvate water when exposed to the air. The temperature of removal of solvate water molecules up to 160°C and removal of organic moieties (coordinated or cationic) after 280°C, depending on nature of organic part is quite common for cluster chemistry [40][61].

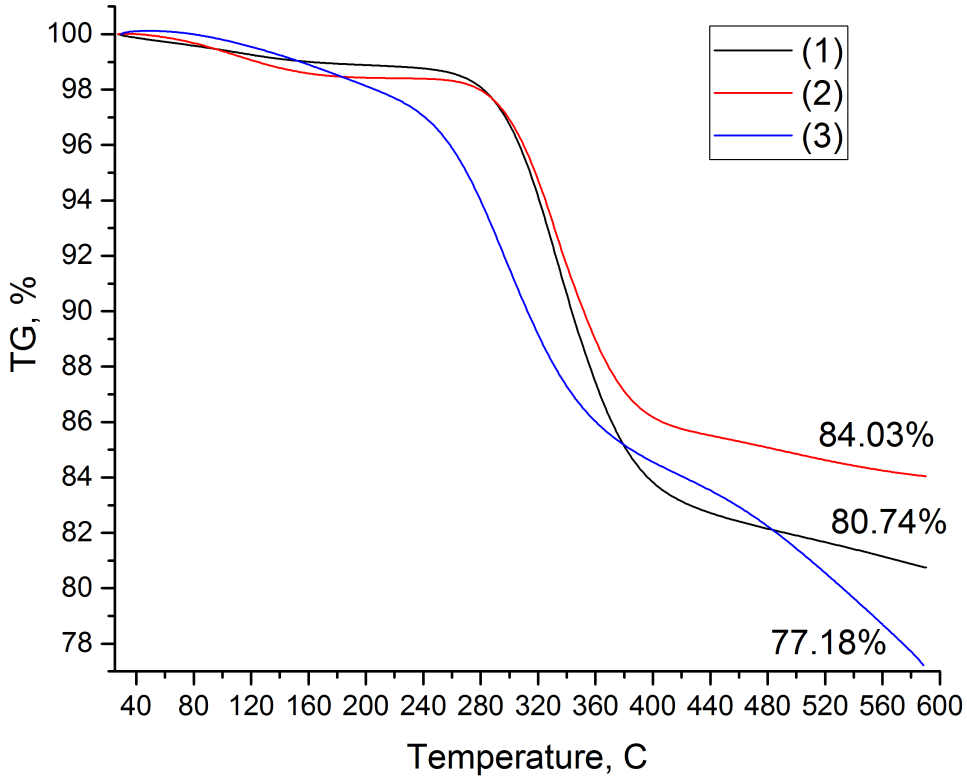

Figure 7. Thermal decomposition of compounds (**1**)–(**3**) (TG curves).

3 Conclusions

It is interesting to note that to date, the rationalization of the dimensionality of the obtained H-bonded molecular networks involving $[Re_6Q_8(CN)_6]^{4-}$ (Q = S, Se or Te) and $[Re_6S_8(CN)_4(H_2O)_2]^{2-}$ clusters has never been described in the literature. Through these examples, this is the first attempts involving such cyano-based metallo clusters embedded in reproducible H-bonded networks. We have previously shown [38],[39] that the molecular recognition between flexible bis-amidinium moieties and $[Re_6S_8(CN)_6]^{4-}$ clusters was effective and leads to robust luminescent H bonded networks. In this work, we went a step further, by using two types of $[Re_6Q_8(CN)_6]^{4-}$ (Q = S or Se) and $[Re_6S_8(CN)_4(OH)_2]^{4-}$ anions and a rigid organic H bond donor 1,4- diamidiniumbenzene (H_2DAB^{2+}), and we demonstrated the reliability and reproducibility of the formed 2D H bonded network of formula $(H_2DAB)_2[Re_6Q_8(CN)_6]\cdot nH_2O$ (Q = S, n = 2,5 (**1**) or Q = Se, n = 2 (**2**)) involving water molecules. In addition, by choosing cation presenting additional H bond acceptor/donor ($[Re_6S_8(CN)_4(OH)_2]^{4-}$) a diamond-like 3D H bonded compound of formula $(HDAB)_2[Re_6S_8(CN)_4(H_2O)_2]\cdot 7H_2O$ where a monocation was observed.

These results validate the robustness of our approach to combine cluster metallo-cyano based compounds as H bond acceptors and charged H bond donors for the formation of molecular compounds of controlled dimentionality. Other compounds are under investigation.

Credit authorship contribution statement

Declaration of competing interest

All authors have given approval to the final version of the manuscript.

Acknowledgments

Financial supports from the University of Strasbourg and the CNRS are acknowledged. A. Ledneva thanks program "Mechnikov" supporting mobility of scientists (French Embassy in Moscow). A. Ledneva and N.G Naumov also thank Ministry of Science and Higher Education of the Russian Federation.

4 References

[1] K. Rissanen, Halogen bonded supramolecular complexes and networks, CrystEngComm, 10 (2008) 1107-1113, 10.1039/B803329N.

[2] M. Saccone, L. Catalano, Halogen Bonding beyond Crystals in Materials Science, J. Phys. Chem. B, 123 (2019) 9281-9290, 10.1021/acs.jpcb.9b07035.

[3] M.C. Etter, Encoding and Decoding Hydrogen-Bond Patterns of Organic-Compounds, Acc. Chem. Res., 23 (1990) 120-126, 10.1021/ar00172a005.

[4] M.D. Ward, Design of crystalline molecular networks with charge-assisted hydrogen bonds, Chem Commun, (2005) 5838-5842, 10.1039/B513077H.

[5] L. Chen, B. Zhang, L. Chen, H. Liu, Y. Hu, S. Qiao, Hydrogen-bonded organic frameworks: design, applications, and prospects, Mater. Adv., 3 (2022) 3680-3708, 10.1039/D1MA01173A.

[6] Y. Liu, G. Chang, F. Zheng, L. Chen, Q. Yang, Q. Ren, Z. Bao, Hybrid Hydrogen-Bonded Organic Frameworks: Structures and Functional Applications, Chem. Eur. J., 29 (2023) e202202655, 10.1002/chem.202202655.

[7] S.A. Dalrymple, M. Parvez, G.K.H. Shimizu, Supramolecular encapsulation of hexaaquo metal ions by second sphere coordination, Chem Commun, (2001) 2672-2673, 10.1039/B110129N.

[8] S. Ferlay, M.W. Hosseini, Molecular Tectonics: Design of Hybrid Networks and Crystals Based on Charge-Assisted Hydrogen Bonds, in: P. Samori, F. Cacialli (Eds.) Functional Supramolecular Architectures, WILEY-VCH Verlag & Co. KGaA, 2011, pp. 195-232, 10.1002/9783527689897.ch07.

[9] I. Cvrtila, V. Stilinović, New Tricks by Old Anions: Hydrogen Bonded Hexacyanoferrous Anionic Networks, Cryst Growth Des, 17 (2017) 6793-6800, 10.1021/acs.cgd.7b01363.

[10] L. Wang, W. Wang, D. Guo, A. Zhang, Y. Song, Y. Zhang, K. Huang, Design and syntheses of hybrid supramolecular architectures: based on $[Fe(C_2O_4)3]^{3-}$ metallotectons and diverse organic cations, CrystEngComm, 16 (2014) 5437-5449, 10.1039/C4CE00357H.

[11] I. Imaz, A. Thillet, J.-P. Sutter, Charge-Assisted Hydrogen-Bonded Assemblage of an Anionic $\{M(C_2O_4)_4\}^{4-}$ Building Unit and Organic Cations: A Versatile Approach to Hybrid Supramolecular Architectures, Cryst Growth Des, 7 (2007) 1753-1761, 10.1021/cg060905+

[12] E.V. Alexandrov, A.V. Virovets, V.A. Blatov, E.V. Peresypkina, Topological Motifs in Cyanometallates: From Building Units to Three-Periodic Frameworks, Chem Rev, 115 (2015) 12286-12319, 10.1021/acs.chemrev.5b00320.

[13] S. Ferlay, O. Felix, M.W. Hosseini, J.M. Planeix, N. Kyritsakas, Second sphere supramolecular chirality: racemic hybrid H-bonded 2-D molecular networks, Chem Commun, (2002) 702-703, 10.1039/B111207B.

[14] S. Ferlay, V. Bulach, O. Felix, M.W. Hosseini, J.M. Planeix, N. Kyritsakas, Molecular tectonics and supramolecular chirality: rational design of hybrid 1-D and 2-D H-bonded molecular networks based on bis-amidinium dication and metal cyanide anions, CrystEngComm, 4 (2002) 447-453, 10.1039/b203336b.

[15] P. Dechambenoit, S. Ferlay, M.W. Hosseini, J.-M. Planeix, N. Kyritsakas, Molecular tectonics: control of packing of hybrid 1-D and 2-D H-bonded molecular networks formed between bisamidinium dication and cyanometallate anions, New J Chem, 30 (2006) 1403-1410, 10.1039/b606265m.

[16] P. Dechambenoit, S. Ferlay, N. Kyritsakas, M.W. Hosseini, Molecular Tectonics: Control of Reversible Water Release in Porous Charge-Assisted H-Bonded Networks, J Am Chem Soc, 130 (2008) 17106-17113, 10.1021/ja806916t.

[17] C. Paraschiv, S. Ferlay, M.W. Hosseini, V. Bulach, J.M. Planeix, Molecular tectonics: design of luminescent H-bonded molecular networks, Chem Commun, (2004) 2270-2271, 10.1039/b410459p.

[18] P. Dechambenoit, S. Ferlay, N. Kyritsakas, M.W. Hosseini, Molecular tectonics: control of packing of luminescent networks formed upon combining bisamidinium tectons with dicyanometallates, CrystEngComm, 13 (2011) 1922-1930, 10.1039/c0ce00607f.

[19] P. Braunstein, Metal clusters in Chemistry, Willey-VCH, New York, 1999.

[20] N.G. Naumov, A.V. Virovets, M.N. Sokolov, S.B. Artemkina, V.E. Fedorov, A novel framework type for inorganic clusters with cyanide ligands: Crystal structures of $Cs_2Mn_3[Re_6Se_8(CN)_6]_2\cdot 15H_2O$ and $(H_3O)_2Co_3[Re_6Se_8(CN)_6]_2\cdot 14.5H_2O$, Angew Chem Int Edit, 37 (1998) 1943-1945, 10.1002/(SICI)1521-3773(19980803)37:13/14<1943::AID-ANIE1943>3.0.CO;2-Q.

[21] M.P. Shores, L.G. Beauvais, J.R. Long, Cluster-expanded Prussian blue analogues, J Am. Chem. Soc., 121 (1999) 775-779, 10.1021/ja983530s.

[22] V.E. Fedorov, N.G. Naumov, Y.V. Mironov, A.V. Virovets, S.B. Artemkina, O.A. Efremova, U.-H. Peak, Inorganic coordination polymers based on chalcocyanyde cluster complexes, J. Struct. Chem., 43 (2002) 669-684, 10.1023/A:1022060806724.

[23] N.G. Naumov, A.V. Virovets, N.V. Podberezskaya, V.E. Fedorov, Synthesis and crystal structure of $K_4[Re_6Se_8(CN)_6]\cdot 3.5H_2O$, J Struct Chem, 38 (1997) 857-862, 10.1007/BF02763902.

[24] Y.V. Mironov, J.A. Cody, T.E. Albrecht-Schmitt, J.A. Ibers, Cocrystallized mixtures and multiple geometries: Syntheses, structures, and NMR spectroscopy of the Re_6 clusters $[NMe_4]_4[Re_6(Te_{8-n}Se_n)(CN)_6]$ (n=0-8), J Am Chem Soc, 119 (1997) 493-498, 10.1021/ja962264k.

[25] L.G. Beauvais, M.P. Shores, J.R. Long, Cyano-Bridged Re_6Q_8 (Q = S, Se) Cluster-Metal Framework Solids: A New Class of Porous Materials, Chem Mater, 10 (1998) 3783-3786, 10.1021/cm980564q.

[26] T. Yoshimura, S. Ishizaka, Y. Sasaki, H.B. Kim, N. Kitamura, N.G. Naumov, M.N. Sokolov, V.E. Fedorov, Unusual capping chalcogenide dependence of the luminescence quantum yield of the hexarhenium(III) cyano complexes $[Re_6(\mu_3\text{-}E)_8(CN)_6]^{4-}$, $E^{2-} = Se^{2-} > S^{2-} > Te^{2-}$, Chem Lett, (1999) 1121-1122, 10.1246/cl.1999.1121.

[27] N.G. Naumov, A.Y. Ledneva, S.J. Kim, V.E. Fedorov, New trans-$[Re_6S_8(CN)_4L_2]^{n-}$ Rhenium Cluster Complexes: Syntheses, Crystal Structures and Properties, J Clust Sci, 20 (2009) 225-239, 10.1007/s10876-009-0233-x.

[28] Y.V. Mironov, K.A. Brylev, S.J. Kim, S.G. Kozlova, N. Kitamura, V.E. Fedorov, Octahedral cyanohydroxo cluster complex trans-$[Re_6Se_8(CN)_4(OH)_2]^{4-}$: Synthesis, crystal structure, and properties, Inorg Chim Acta, 370 (2011) 363-368, 10.1016/j.ica.2011.01.110.

[29] A.Y. Ledneva, K.A. Brylev, A.I. Smolentsev, Y.V. Mironov, Y. Molard, S. Cordier, N. Kitamura, N.G. Naumov, Controlled synthesis and luminescence properties of trans-$[Re_6S_8(CN)_4(OH)_{2-n}(H_2O)_n]^{n-4}$ octahedral rhenium(III) cluster units (n=0, 1 or 2), Polyhedron, 67 (2014) 351-359, 10.1016/j.poly.2013.09.015.

[30] N.G. Naumov, E.V. Ostanina, A.V. Virovets, M. Schmidtman, A. Müller, V.E. Fedorov, 23-Electron Re6 metal clusters: syntheses and crystal structures of $(Ph_4P)_3[Re_6S_8(CN)_6]$, $(Ph_4P)_2(H)[Re_6Se_8(CN)_6]\cdot 8H_2O$, and $(Et_4N)_2(H)[Re_6Te_8(CN)_6]\cdot 2H_2O$, Russ Chem Bull, 51 (2002) 866-871, 10.1023/A:1016053305232.

[31] M. Emirdag-Eanes, J.A. Ibers, Conversion of a Re(IV) Tetrahedral Cluster to a Re(III) Octahedral Cluster: Synthesis of $[(CH_3)C(NH_2)_2]_4[Re_6Se_8(CN)_6]$ by a Solvothermal Route, Inorg Chem, 41 (2002) 6170-6171, 10.1021/ic020433y.

[32] K.A. Brylev, P. Sekar, N.G. Naumov, V.E. Fedorov, J.A. Ibers, Reactions of transition-metal cations with $[Re_6Te_8(CN)_6]^{4-}$: syntheses and structures of $[Zn(NH_3)_4]_2[Re_6Te_8(CN)_6]$, $[\{Co(NH_3)_5\}_2Re_6Te_8(CN)_6]\cdot 4H_2O$, and $[\{Ni(NH_3)_5\}_2Re_6Te_8(CN)_6]\cdot 4H_2O$, Inorg Chim Acta, 357 (2004) 728-732, 10.1016/j.ica.2003.06.014.

[33] S.A. Baudron, P. Batail, C. Coulon, R. Clerac, E. Canadell, V. Laukhin, R. Melzi, P. Wzietek, D. Jerome, P. Auban-Senzier, S. Ravy, $(EDT\text{-}TTF\text{-}CONH_2)_6[Re_6Se_8(CN)_6]$, a metallic Kagome-type organic-inorganic hybrid compound: Electronic instability, molecular motion, and charge localization, J Am Chem Soc, 127 (2005) 11785-11797, 10.1021/ja0523385.

[34] S. Carlsson, L. Zorina, D.R. Allan, J.P. Attfield, E. Canadell, P. Batail, Robust Dirac-Cone Band Structure in the Molecular Kagome Compound $(EDT\text{-}TTF\text{-}CONH_2)_6[Re_6Se_8(CN)_6]$, Inorg Chem, 52 (2013) 3326-3333, 10.1021/ic302790m.

[35] M.V. Bennett, L.G. Beauvais, M.P. Shores, J.R. Long, Expanded Prussian Blue Analogues Incorporating $[Re_6Se_8(CN)_6]^{3-/4-}$ Clusters: Adjusting Porosity via Charge Balance, J Am Chem Soc, 123 (2001) 8022-8032, 10.1021/ja0110473.

[36] M.S. Tarasenko, E.O. Golenkov, N.G. Naumov, N.K. Moroz, V.E. Fedorov, Unusual H-bonding in novel cyano-cluster polymeric hydrates $[(H)\{Ln(H_2O)_4\}\{Re_6S_8(CN)_6\}]\cdot 2H_2O$ (Ln = Yb, Lu), Chem. Comm. (2009), 2655-2657 10.1039/B820722D.

[37] M.J. Suh, V. Vien, S. Huh, Y. Kim, S.J. Kim, Mesolamellar phases containing $[Re_6Q_8(CN)_6]^{4-}$ (Q = Te, Se, S) cluster anions, Eur J Inorg Chem, (2008) 686-692, 10.1002/ejic.200701125.

[38] A. Ledneva, S. Ferlay, N.G. Naumov, M. Mauro, S. Cordier, N. Kyritsakas, M.W. Hosseini, Hydrogen bonded networks based on hexarhenium(iii) chalcocyanide cluster complexes: structural and photophysical characterization, New J Chem, 42 (2018) 11888-11895, 10.1039/C8NJ02310G.

[39] A.Y. Ledneva, N.G. Naumov, N. Kyritsakas, S. Ferlay, Tuning the dimensionality of H bonded networks using different chalcogen atoms in $[Re_6Q_8(CN)_6]^{4-}$ (Q = S, Se) clusters, J Struct Chem, 5 (2024) 126941, 10.26902/JSC_id126941

[40] A.I. Smolentsev, A.V. Ermolaev, Y.V. Mironov, Hydrogen bonding in two ionic complexes built from octahedral rhenium(III) chalcocyanohydroxo cluster anions and tris(ethylenediamine)nickel(II) cations, $[Ni(en)_3]_2[Re_6S_8(CN)_4(OH)_2]\cdot 5.5H_2O$ and $[Ni(en)_3]_2[Re_6Se_8(CN)_4(OH)_2]\cdot 10H_2O$, J Mol Struct, 1014 (2012) 57-62, 10.1016/j.molstruc.2012.02.005.

[41] A.V. Ermolaev, A.I. Smolentsev, Y.V. Mironov, Synthesis and physicochemical studies of the compounds based on $[Ni(Dien)(NH_3)_3]^{2+}$ and $[Ni(Trien)(NH_3)_2]^{2+}$ cations and $[Re_6Se_8(CN)_4(OH)_2]^{4-}$ octahedral cluster anion, Russ J Coord Chem+, 42 (2016) 730-736, 10.1134/S1070328416110026.

[42] G. Xing, I. Bassanetti, T. Ben, S. Bracco, P. Sozzani, L. Marchiò, A. Comotti, Multifunctional Organosulfonate Anions Self-Assembled with Organic Cations by Charge-Assisted Hydrogen Bonds and the Cooperation of Water, Cryst Growth Des, 18 (2018) 2082-2092, 10.1021/acs.cgd.7b01538.

[43] G. Xing, I. Bassanetti, S. Bracco, M. Negroni, C. Bezuidenhout, T. Ben, P. Sozzani, A. Comotti, A double helix of opposite charges to form channels with unique CO_2 selectivity and dynamics, Chem. Sci., 10 (2019) 730-736, 10.1039/C8SC04376K.

[44] S. Zheng, L. Li, L. Chen, Z. Fan, F. Xiang, Y. Yang, Z. Zhang, S. Xiang, Two Water Stable Phosphate-Amidinium Based Hydrogen-Bonded Organic Framework with Proton Conduction, Z. anorg. Allg. Chem. 648 (2022) e202200031, 10.1002/zaac.202200031.

[45] A.R.Y. Almuhana, G.R.F. Orton, C. Rosenberg, N.R. Champness, Photoinduced radical formation in hydrogen-bonded organic frameworks, Chem Commun, 60 (2024) 452-455, 10.1039/D3CC05236B.

[46] S. Ferlay, P. Dechambenoit, N. Kyritsakas, M.W. Hosseini, Molecular tectonics: tuning the dimensionality and topology of extended cyanocuprate networks using a bisamidinium cation, Dalton T, 42 (2013) 11661-11671, 10.1039/C3DT51252E.

[47] G.-L. Song, H.-J. Zhu, L. Chen, S. Liu, Z.-H. Luo, Novel Disubstituted Phenylene-Linked Bis-imidazole Derivatives: Facile Synthesis and Optical Properties, Helvetica Chimica Acta, 93 (2010) 2397-2405, 10.1002/hlca.201000014.

[48] N.G. Naumov, S.B. Artemkina, A.V. Virovets, V.E. Fedorov, Adjustment of dimensionality in covalent frameworks formed by Co^{2+} and rhenium cluster chalcocyanide $[Re_6S_8(CN)_6]^{4-}$, Solid State Sci, 1 (1999) 473-482, 10.1016/S1293-2558(00)80100-4.

[49] G. te Velde, F.M. Bickelhaupt, E.J.Baerends, C. Fonseca Guerra, S.J.A. van Gisbergen, J.G. Snijders, T. Ziegler, Chemistry with ADF. J. Comput. Chem. 22 (2001) 931-967, 10.1002/jcc.1056.

[50] E. Van Lenthe, E.J. Baerends, Optimized Slater-type basis sets for the elements 1-118. J. Comput. Chem. 24 (2003) 1142-1156, 10.1002/jcc.10255

[51] J.P.Perdew Density-functional approximation for the correlation energy of the inhomogeneous electron gas. Phys. Rev. B 33 (1986) 8822-8824, 10.1103/PhysRevB.33.8822

[52] E. van Lenthe, A. Ehlers, E.-J. Baerends, Geometry optimizations in the zero order regular approximation for relativistic effects. J. Chem. Phys. 110 (1999) 8943-8953, 10.1063/1.478813

[53] G. Sheldrick, A short history of SHELX, Acta Cryst A, 64 (2008) 112-122, 10.1107/S0108767307043930.

[54] G. Sheldrick, Crystal structure refinement with SHELXL, Acta Cryst. C, 71 (2015) 3-8, 10.1107/S2053229614024218.

[55] B.A.I. M86-EXX229V1 APEX3 User Manual", Madison, USA, (2016).

[56] A. L. Spek, Acta Cryst. D65 (2009) 148-155 10.1107/S090744490804362X

[57] PowderCell for Windows, version 2.4 8.03.2000 W.Kraus, G.Nozle Federal Institure for materials research and testing, Berlin, Germany

[58] N.G. Naumov, A.V. Virovets, V.E. Fedorov, Octahedral rhenium(III) chalcocyanide cluster anions: Synthesis, structure, and solid state design, J. Struct. Chem, 41 (2000) 499-520, 10.1007/BF02742011.

[59] L. Feng, Y. Yuan, B. Yan, T. Feng, Y. Jian, J. Zhang, W. Sun, K. Lin, G. Luo, N. Wang, Halogen hydrogen-bonded organic framework (XHOF) constructed by singlet open-shell diradical for efficient photoreduction of U(VI). Nat Commun 13, (2022). 10.1038/s41467-022-29107-9

[60] M. Jokic, M. Bajic, M. Zinic, B. Peric, B. Kojic-Prodic, Benzdiamidine Acta Cryst. C57 (2001) 1354-1355 10.1107/S010827010101438X

[61] A.V. Ermolaev, A. I. Smolentsev, Y. V. Mironov Use of $[Re_6Q_8(CN)_6]^{4-}$ (Q=S, Se, Te) cluster anions and Cu(I) cationic complexes with 2,2′-bipyridine for the construction of new cyano-bridged coordination compounds, Polyhedron 102, (2015) 417-423, 10.1016/j.poly.2015.10.024